

# Cranial cruciate ligament structure in relation to the tibial plateau slope and intercondylar notch width in dogs

Michal Kyllar<sup>1,2,\*</sup>, Petr Čížek<sup>1</sup>

<sup>1</sup>Department of Anatomy, Histology and Embryology, Faculty of Veterinary Medicine, University of Veterinary and Pharmaceutical Sciences Brno, 612 42 Brno, Czech Republic

<sup>2</sup>Companion Care, Broadstairs CT10 2RQ, United Kingdom

Cranial cruciate ligament (CCL) rupture is one of the most common orthopedic conditions in dogs. The pathogenesis of CCL rupture is not fully described and remains to be elucidated fully. Several hypotheses have been proposed to explain the etiology of these changes. The objective of this study was to investigate structural changes in the CCL in relation to the tibial plateau angle (TPA) and the intercondylar notch (ICN) width in dogs. Fifty-five skeletally mature dogs were included in this study. ICN width and TPA measurements were obtained from intact CCL stifles. Samples of the CCL, caudal cruciate ligament (CaCL), and femoral head ligament (FHL) were harvested and stained for routine histological and immunohistochemical analysis. Microscopic changes in the ligaments were observed and were found to correlate with the TPA and ICN width values. The degree of structural changes within the CCL was observed to correlate with an increasing TPA and a narrowing ICN width. Changes in the CCL are likely to be caused by excessive forces acting through the ligament in stifles with a high TPA. Chondroid metaplasia of the CCL is an adaptation to abnormal mechanics within the stifle joint caused by altered bone morphology.

**Keywords:** arthritis, cranial cruciate ligament, stifle

## Introduction

Cranial cruciate ligament (CCL) rupture is one of the most common orthopedic conditions affecting the stifle joint in dogs [11,20,38]. The pathogenesis of its rupture is not fully described and remains to be elucidated fully. The majority of canine CCL ruptures are thought to be secondary to chronic degenerative changes within the ligament [14,15]. Several hypotheses have been proposed to explain the etiology of these changes. They can be divided into two basic components—biological and biomechanical [8]. The biologic components include immune-mediated diseases, arthritis, hormonal influences, impaired synthesis turnover of extracellular matrix, and apoptosis [2,3,13,17-19,21,29,30,33,35]. The biomechanical components include morphological deformities of the proximal tibia and distal femur, malalignment, altered kinematics or distorted joint contact areas, and pressure [1,4,5,9,10,16,22,23,25,31,32,34,37,39]. Even though many of these components have been implicated as causes of cruciate ligament rupture, it is unclear whether a single component or a combination of components is the reason for CCL rupture.

Therefore, all these factors should be considered contributors to a multifactorial process during organ failure [8]. CCL rupture results in joint instability and a subsequent progression of osteoarthritic (OA) changes in the stifle joint [19].

The caudal cruciate ligament (CaCL) has received less attention in the literature as pathology in the form of rupture is rare except in cases of multi-ligament ruptures during severe trauma to the stifle joint. The CaCL prevents caudal translation and tibial subluxation after lift-off [28].

The femoral head ligament (FHL) is another intra-articular ligament, the function of which has not been fully elucidated in adult dogs. Hip joint laxity and subsequent development of osteoarthritis is a common orthopedic condition affecting dogs [24]. The function of the FHL in unstable hip joints has not been thoroughly evaluated, and one current report attributes no role of the FHL in the development of hip joint laxity [27].

Microscopic analysis of the CCL has not detected any differences in cell population, morphology, or extracellular matrix status between the CCL and other ligaments [2,27,40]. Typical CCL fibroblasts have a prolonged oval shape, and they are sometimes located in lacunae [7,19]. This structural feature

Received 11 Apr. 2018, Revised 29 May 2018, Accepted 10 Jun. 2018

\*Corresponding author: Tel: +44-420604206455; Fax: +44-01843608431; E-mail: [kyllarm@vfu.cz](mailto:kyllarm@vfu.cz)

Journal of Veterinary Science · © 2018 The Korean Society of Veterinary Science. All Rights Reserved.

This is an Open Access article distributed under the terms of the Creative Commons Attribution Non-Commercial License (<http://creativecommons.org/licenses/by-nc/4.0>) which permits unrestricted non-commercial use, distribution, and reproduction in any medium, provided the original work is properly cited.

pISSN 1229-845X

eISSN 1976-555X

of the CCL was considered by some authors as a pathological feature [19] and by others as a physiological condition typical of intra-articular ligaments [7]. To our knowledge, the microscopic structure of the FHL in dogs has not been described. Information on the description of the human FHL and on the characterization of a healthy ligament structure is currently limited [27].

Despite the clinical importance of cruciate ligament disease in the dog, few studies have focused on histological and immunohistochemical analyses of cruciate ligaments in relation to the biomechanical features of the stifle joint. Vasseur *et al.* [36] reported a correlation between deterioration in the mechanical properties of the intact CCL and the degree of adaptive or age-related histological changes in ligament structure in larger dogs. Few studies have focused on the relationship between the biomechanical and biological factors related to possible CCL rupture [5,36]. Chondroid metaplasia of ligamentous tissue has been described as a distinct feature in both intact and ruptured CCL specimens, but its development and contribution to ligament rupture remain to be elucidated [5].

The purpose of this study was to determine and compare the microscopic structure of intra-articular ligaments (CCL, CaCL, and FHL) focusing on chondroid metaplasia within the CCL. The CaCL and FHL in this study serve as a “control tissues” as they are in the same intra-articular environment as the CCL. Furthermore, we investigated the relationship between the structure of the CCL and selected morphological features of the proximal tibia (tibial plateau angle, TPA) and the distal femur (intercondylar notch, ICN). We hypothesized that structural changes of the CCL arise in relation to the degree of TPA and size of the ICN. Moreover, we expect that these changes will be different from those of other intra-articular ligaments.

## Materials and Methods

### Animals

Fifty-five skeletally mature mongrel dogs (> 12 months old) were used in this study (28 females and 27 males; Table 1). Dogs were euthanized for reasons unrelated to this study. Written consent of the owners for the use of the cadavers in this study

**Table 1.** Characteristics of the study population

|            | CCL       | CaCL      | FHL       |
|------------|-----------|-----------|-----------|
| Gender (n) |           |           |           |
| Male       | 26        | 28        | 9         |
| Female     | 26        | 22        | 6         |
| Age (yr)   | 6.2 ± 3.5 | 6.0 ± 3.9 | 3.1 ± 2.8 |

Data are presented as mean ± SD. CCL, cranial cruciate ligament; CaCL, caudal cruciate ligament; FHL, femoral head ligament.

was obtained. Handling of the study was carried out according to the guidelines of the Branch Commission for Animal Welfare of the Ministry of Agriculture of the Czech Republic (PP59-2014 UVP). All dogs had a full clinical history and only dogs between 15 and 30 kg, free of OA changes in the stifle or hip joint, and without previous trauma or surgery in the investigated joints were included in the study. Presence or absence of OA signs was confirmed radiographically. Use of anti-inflammatory medications within the last month prior to euthanasia was an exclusion criterion.

Fifty-two CCL samples, fifty CaCL samples, and fifteen FHL samples were obtained from the investigated joints. Three samples of CCL, five samples of CaCL and forty samples of FHL were excluded due to macroscopically apparent partial rupture or incomplete sampling (Table 1).

### Radiography

Radiographs of each stifle joint were taken immediately following euthanasia. Craniocaudal and mediolateral projections were obtained to assess stifle conformity, the presence of OA changes, and to assess tibial plateau slope by measuring the TPA [32].

### Ligaments

Specimens of entire CCLs, CaCLs, and FHLs were harvested from corresponding joints unilaterally. Incomplete ligaments or ligaments with macroscopically visible ruptures were excluded from the study. The ligaments were removed from the joints by incising their proximal and distal attachments, and they were marked with suture material of different colors for later identification of their orientation. The areas of impingement (contact of the ligament with the bone) of the ICN on each CCL were marked with a permanent marker. Ligament samples were fixed in 4% formaldehyde immediately after their collection and stored for further investigation.

### Intercondylar notch investigation

Complete femurs were prepared by using a maceration procedure. Several measurements of the ICN were taken by using digital calipers as described by Fitch *et al.* [12]. The cranial, central, and caudal notch widths were measured and their indices (notch width index [NWI]) and the overall NWI for each stifle were calculated as described previously [5].

### Tissue specimen processing

Fixed specimens were washed in water, dehydrated through an ethanol series, and embedded in paraffin wax. Serial longitudinal histological sections were prepared (thickness 5 µm) with preservation of orientation. Sections were mounted on super-frost glass slides for histological staining, and alternative slides were maintained for immunohistochemical analysis.

### Histological evaluation

Specimens of CCLs, CaCLs, and FHLs were stained with H&E to evaluate cell population and morphology, and with alcian blue to evaluate the proteoglycan content of the extracellular matrix. All samples were evaluated by a single investigator (P. Čížek). Sections were examined for evidence of chondroid metaplasia (*e.g.*, loss of characteristic spindle-shaped fibroblasts with transformation into ovoid or round nuclei with normal or clonal appearance; formation of perinuclear 'halo' areas) and matrix degradation (*e.g.*, loss of typical collagen fiber organization; increased amount of proteoglycans; woven appearance of collagen fiber, and fiber disorganization). Degrees of chondroid metaplasia and matrix degradation were scored according to Barrett *et al.* [2] on a scale from 1 to 5 (1, no changes; 2, mild changes in a small area of the ligament; 3, moderate changes; 4, severe changes; and 5, severe diffuse changes).

### Immunohistochemical detection

Alternative tissue sections were deparaffinized by xylene and dehydrated by using ethanol (100%, 96%, and 70%). Antigen retrieval was performed for 20 min in citrate buffer in the water bath (97°C) followed by cooling at room temperature for an additional 20 min. Sections were treated with H<sub>2</sub>O<sub>2</sub> (3% in phosphate-buffered saline [PBS]) for 10 min to inactivate endogenous peroxidases. Fc receptors were blocked with normal goat serum (1.5% solution, LSAB kit; Dako, Denmark) for 30 min. The primary antibodies S100 (ab66041; Abcam, United Kingdom) or matrix metalloproteinase-2 (MMP-2) (ab37150; Abcam) were diluted 1:100 in antibody diluents (Dako). After an incubation time of 1 h at 37°C and washing in PBS, sections were incubated with biotinylated anti-rabbit antibody (Vectastain ABC kit; Vector Laboratories, USA) diluted 1:200 in PBS for 30 min. Avidin-biotin complex (Vectastain ABC kit) was applied for 30 min, and products were visualized with diaminobenzidine. Color development was stopped when the positive control slides showed a clearly visible signal (20–30 sec). Sections were counterstained with hematoxylin for 1 to 2 min, dehydrated by ethanol (70%, 96%, and 100%), and after a xylene wash were embedded with Glycergel (Dako). Negative control slides omitting the primary antibody were included in each batch. Tissues were evaluated and photographed (microscope: Olympus BX-43 [Olympus, Japan]; camera system: Olympus XC-10IR [Olympus]). Immunohistochemical stains were scored in a manner similar to that used for histological staining, and the number of S100-positive cells and MMP-2-positive cells were counted on each slide. If more than 200 cells were counted, then the result was recorded as too numerous to count. Specimens were divided into two groups based on TPA: < 24° and > 24° based on suspected breed predisposition to CCL rupture and the associated tibial plateau slope [38].

### Statistical analysis

Kruskal-Wallis ANOVA and Mann-Whitney *U* test were used to evaluate differences between groups (CCL TPA < 24°, CCL TPA > 24°, CaCL, FHL). Dependent variables included number of S100-positive cells, number of MMP-2-positive cells, degree of chondroid metaplasia, and degree of matrix degeneration. For all comparisons, values of *p* < 0.05 were

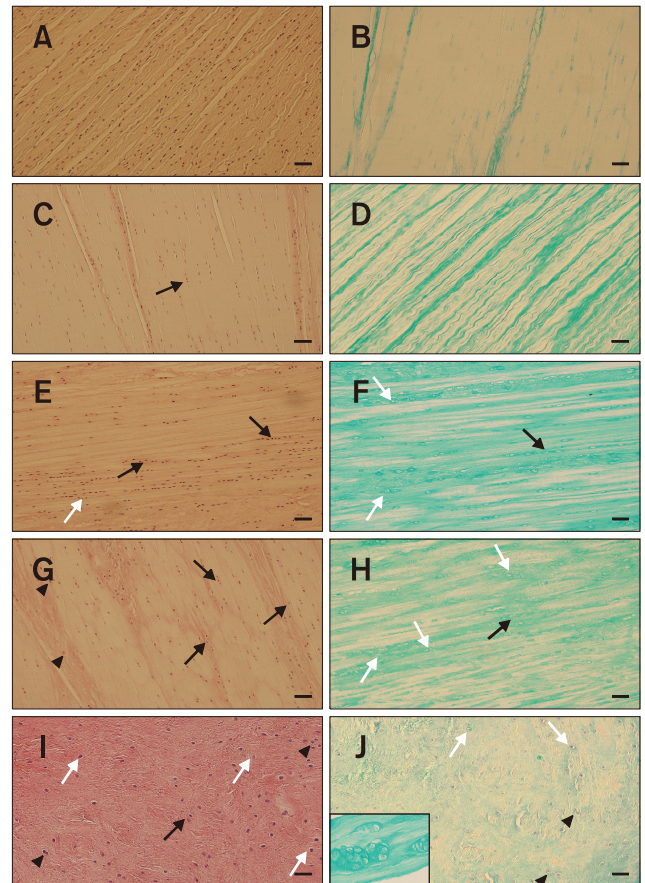


**Fig. 1.** Histological appearance of the cranial cruciate ligament with different structural changes. (A and B) Histological appearance of a normal cranial cruciate ligament showing typical fibroblast orientation with a spindle-shaped appearance, regular fascicular structure, and pale interfascicular areas. (C–F) Mild fibroblast transformation of the nuclei into an ovoid to round shape, some columnar chondroid transformation (black arrows) and formation of perinuclear halo (white arrows), loss of even distribution of the fibroblasts within the ligament, regular fascicular structure, and increased mucopolysaccharide content (alcian blue/periodic acid-Schiff [AC-PAS] stain). (G–J) Significant chondroid metaplasia with the formation of columns (black arrows) and clones of transformed fibroblasts (black arrowheads and inset in panel J), irregular fascicular network, and a significant increase in mucopolysaccharides (AC-PAS). White arrows, perinuclear halo. H&E stain (A, C, E, G, and I). AC-PAS stain (B, D, F, H, and J). Scale bars = 100  $\mu$ m (A–J). 400 $\times$  (inset in panel J).

considered significant. The Spearman rank correlation method was used to examine possible associations between TPA and histological score within each ligament.

## Results

### Tibial plateau angle measurements

The TPAs ranged from 18° to 36°. Mean TPA in males was 24.3 ± 1.5° (SD) and in females 23.7 ± 1.0°. No significant difference was detected between genders ( $p < 0.05$ ).

### Intercondylar notch width measurements

Cranial NWI was calculated to be 0.12 ± 0.02, central NWI 0.15 ± 0.02, and caudal NWI 0.25 ± 0.03. No significant difference was detected between cranial and central NWI ( $p = 0.18$ ). There was a significant difference between caudal and central NWI, as well as between caudal and cranial NWI ( $p < 0.05$ ). The overall NWI was 0.17 ± 0.09. No significant difference was detected between genders ( $p < 0.05$ ).

### Microscopic changes of cranial cruciate ligaments correlated with increased tibial plateau angle

A variety of microscopic changes in the CCLs, ranging from physiological structure of ligamentous tissue to chondroid metaplasia, were observed. Typical ligaments (grades 0 and 1) contained characteristic spindle-shaped fibroblasts nuclei uniformly distributed throughout the structure of the ligament. Cells were arranged in rows parallel to collagen fibers. This appearance was characteristic for stifles with a TPA less than 24° (panel A in Fig. 1). Some ligaments showed mild shape changes in fibroblast nuclei resulting in a round profile with loss of parallel orientation and an irregular distribution throughout the ligament (grades 2 and 3). Round-shaped fibroblast nuclei were concentrated in the central areas of the ligament in its proximo-distal direction. A perinuclear halo was a typical

feature of ligaments harvested from stifles with TPA of more than 24° (panels C–F in Fig. 1, Table 2). Moderate to severe changes (grades 4 and 5) were characterized by chondroid metaplasia of the fibroblasts mainly in the central part of the ligament. This metaplasia was characterized by the formation of clones, rearrangement of fibroblasts into columns, and fibroblasts located in lacunae (panels G–J in Fig. 1). Structural changes became more apparent with increased TPA (Table 2). Moderately to severely affected ligaments showed loss of parallel collagen fibers with an interwoven appearance (panels G–J in Fig. 1).

The level of alcian blue staining in the CCLs varied from a minimal amount of extracellular matrix in the physiological ligaments (panel B in Fig. 1) to a strong signal in ligaments with chondroid metaplasia (panels F, H, and J in Fig. 1). These changes were typical in ligaments with a TPA of more than 24° (Table 2).

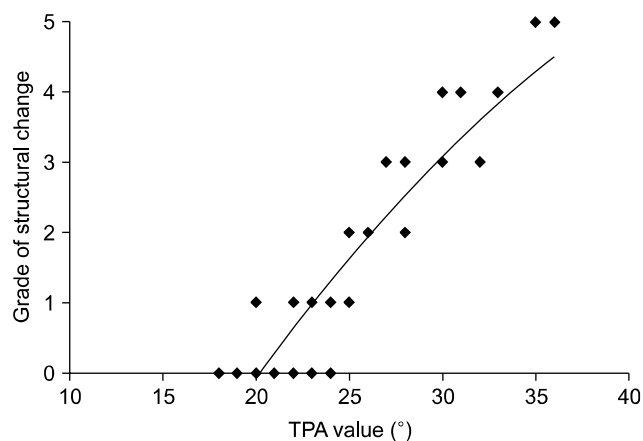


**Fig. 2.** Relationship of structural changes between the cranial cruciate ligament and the tibial plateau angle (TPA).

**Table 2.** Median scores of structural changes in the cranial cruciate ligament, caudal cruciate ligament, and femoral head ligament, and median numbers of S100 and MMP-2-positive cells

| Variable             | CCL              |                  | CaCL             |                  | FHL              |
|----------------------|------------------|------------------|------------------|------------------|------------------|
|                      | TPA < 24°        | TPA > 24°        | TPA < 24°        | TPA > 24°        |                  |
| Chondroid metaplasia | 1.5 <sup>a</sup> | 3.5 <sup>b</sup> | 1 <sup>a</sup>   | 1 <sup>a</sup>   | 0.5 <sup>c</sup> |
| Matrix degeneration  | 0.5 <sup>a</sup> | 3 <sup>b</sup>   | 0.5 <sup>a</sup> | 0.5 <sup>a</sup> | 0.5 <sup>c</sup> |
| S100                 | 0 <sup>a</sup>   | 2 <sup>b</sup>   | 0.5 <sup>a</sup> | 0.5 <sup>a</sup> | 0 <sup>a</sup>   |
| MMP-2                | 0 <sup>a</sup>   | 1.5 <sup>b</sup> | 0.5 <sup>a</sup> | 0.5 <sup>a</sup> | 0 <sup>c</sup>   |
| S100-positive cells  | 10 <sup>a</sup>  | 120 <sup>b</sup> | 20 <sup>a</sup>  | 20 <sup>a</sup>  | 0 <sup>a</sup>   |
| MMP-2-positive cells | 0 <sup>a</sup>   | 180 <sup>b</sup> | 0 <sup>a</sup>   | 0 <sup>a</sup>   | 0 <sup>a</sup>   |

Histological features were scored on a scale from 1 (no evidence) to 5 (severe and diffuse). Numbers of S100-positive cells and MMP-2-positive cells were counted in an entire section of the ligament sample. MMP-2, matrix metalloproteinase-2; CCL, cranial cruciate ligament; CaCL, caudal cruciate ligament; FHL, femoral head ligament; TPA, tibial plateau angle. <sup>a-c</sup>Values in each row with different superscript letters were significantly different ( $p < 0.05$ ).



Moderate to severe changes with chondroid metaplasia and extracellular matrix production of the ligament structure were mainly located in the central part of the ligament in a proximo-distal direction (Fig. 2). All structural changes were mainly apparent at the site of ligament attachment and in the areas that came into contact with the ICN in the center of the ligament (Fig. 3).

### Changes in the caudal cruciate ligament structure resembled changes in the cranial cruciate ligament

The CaCLs exhibited a structure typical of healthy ligamentous tissue with parallel rows of spindle-shaped fibroblasts' nuclei uniformly distributed throughout the ligament. Areas of moderate chondroid metaplasia with increased uptake of alcian blue and disorganization were found in the central part of the ligament that comes into contact with the ICN. Similar changes were observed in the attachment side of the ligament. Chondroid metaplasia was mainly characterized by oval- or round-shaped chondrocyte-like cells with a perinuclear halo. No clones of cells or arrangement into columns were observed. Alcian blue staining was apparent only in areas with chondroid metaplasia. The severity of changes within the ligament reached a

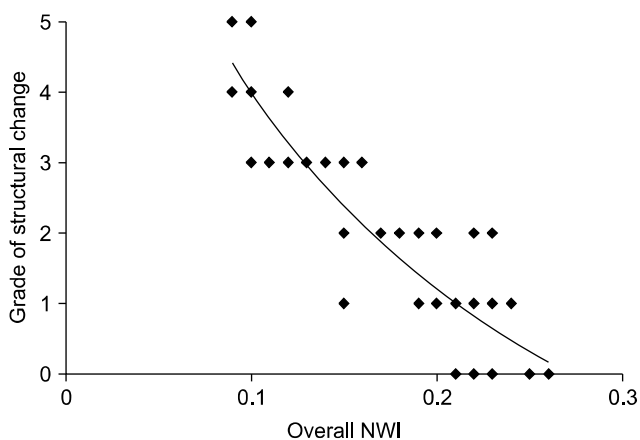


**Fig. 3.** Relationship of structural changes between the cranial cruciate ligament and the overall notch width index (NWI).

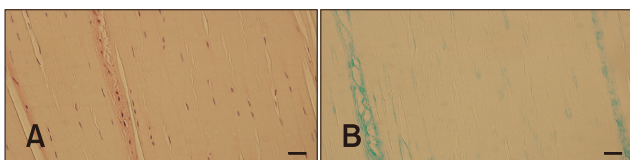


**Fig. 4.** Histological structure of the femoral head ligament showing characteristics of normal ligamentous structure, such as spindle-shaped fibroblasts' nuclei, regular fiber pattern, and minimal staining for mucopolysaccharides. H&E stain (A and B). Scale bars = 100 µm (A and B).

maximum of grade 3 in the CCL (panels A-F in Fig. 1).

### The femoral head ligament did not show morphological alteration

The FHL structure displayed a physiological morphology with spindle-shaped fibroblast nuclei uniformly distributed throughout the ligament with parallel collagen fibers (panel A in Fig. 4). Areas of chondroid metaplasia and disorganization of collagen fibers were localized in the areas of attachment of the ligament. Alcian blue staining was negative to weak (panel B in Fig. 4).

### Expressions of S-100 and MMP2 were colocalized with areas of chondroid metaplasia

The S-100 protein is generally located in cells derived from chondrocytes and other cells. Areas of marked chondroid metaplasia, where perinuclear halos were formed, stained positively for S-100. Typical fibroblasts were negative for S-100 expression. Positive cells were apparent in the CCL, as well as in the CaCL, in all areas with chondroid metaplasia. FHLs showed positive staining for S-100 only in the areas of attachment (Fig. 5).

MMP-2 is involved in tissue degradation and remodeling. Expression of MMP-2 was observed in areas of degeneration where chondroid metaplasia and collagen disruption were present. FHLs did not show positive staining for MMP-2 (Fig. 6).

There were significant differences in degenerative changes scores among the three ligaments ( $p < 0.05$ ; Table 2).

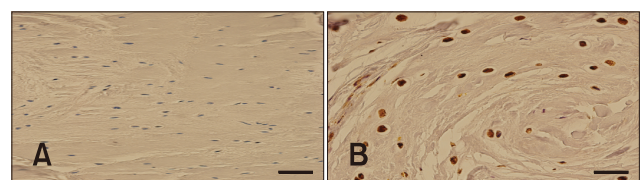


**Fig. 5.** S100 staining of the cranial cruciate ligament. (A) Negative staining of the stifle with a tibial plateau angle (TPA) of 21°. (B) Positive expression of S100 of a stifle with a TPA of 32°. Scale bars = 100 µm (A), 40 µm (B).

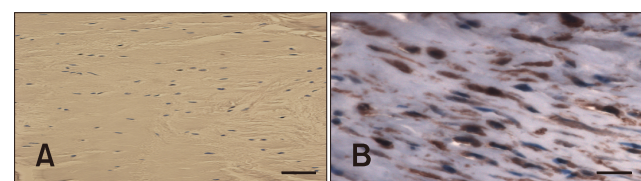


**Fig. 6.** Matrix metalloproteinase-2 (MMP-2) staining of the cranial cruciate ligament. (A) Negative staining of the stifle with a tibial plateau angle (TPA) of 21°. (B) Positive expression of MMP-2 of a stifle with a TPA of 32°. Scale bars = 100 µm (A), 40 µm (B).

Degenerative changes in the structure of the CCLs was strongly correlated with an increasing TPA (Fig. 2) and a narrowing of the anterior ICN width (Fig. 3). There were significant differences in degenerative changes in the CCLs with TPA < 24° compared to those in CCLs with TPA > 24° ( $p < 0.05$ ; Table 2). The median numbers of S-100-positive cells and MMP-2-positive cells from the TPA > 24° group were significantly different from those in the TPA < 24° group. No significant differences in degenerative changes were detected between the CaCL and FHL (Table 2). No significant relationship in TPA, ligament structure, or ICN width was detected when comparing age and gender.

## Discussion

Cruciate ligament disease in dogs can be considered an organ failure in which malfunction of biological or biomechanical components become an initiating factor [8]. The biologic components include inflammation, impaired synthesis and repair of the extracellular matrix, necrosis, and apoptosis [2,3,13]. The biomechanical components can include instabilities of various types, muscle weakness and dysfunction, altered kinematics, and conformational changes [1,4,5,9,10,16]. Our study focused on the assessment of proximal tibia and distal femur morphologies, and their influence on the structure of the CCL. Samples of CaCLs and FHLs were used for structural comparison because of their intra-articular location and, therefore, expected structural similarity.

Previously, TPA has been considered as one of the major contributing factors to abnormal stifle joint biomechanics [28]. However, results in studies focusing on TPA in different breeds of dogs and their relationship to CCL rupture are contradictory [24,26,27,40]. We have found differences in TPAs between different dogs in our study. Nevertheless, the results must be interpreted with caution because we have investigated a limited number of dogs (only mongrels with intact CCLs and within the same weight group).

Width of the ICN is another aspect of the stifle joint that is considered a potential risk factor contributing to CCL rupture [12]. Our study revealed variability in the ICN width within the same weight group of dogs, which is in agreement with the results of a similar study published by Comerford *et al.* [5].

Currently, it is believed that TPA and ICN width may contribute to the process of CCL failure, but they do not appear to be primary casual factors [8]. Structural and/or degenerative changes within the CCLs were compared between different breeds of dogs with or without a predisposition to their rupture [5,7,39]. Degenerative changes were reported as soon as at two years of age [4,36]. However, only a few studies have compared and linked structural changes within the ligament to stifle conformation [5,36]. These studies are not in agreement on what is structurally considered a physiological feature of CCLs

(or their physiological adaptation) and what is already considered a degenerative change [5,36,39]. The microscopic structure of the ligament is defined by well-spaced spindle-shaped fibroblasts, a regular fascicular structure of collagen fibers, and a paler interfascicular area with normal blood vessels [9]. There have also been reports of changes within the ligament of both cellular morphology and the amount and quality of the extracellular matrix [26]. Cellular morphology varies from spindle-shaped to round or ovoid fibroblasts. In progressed degeneration, a perinuclear halo develops, which is considered by some authors as the first sign of chondroid metaplasia [7,19,26]. Extracellular morphology varies from parallel collagen fibers and a pale interfascicular area to a reduced density of collagen fiber staining, collagen crimp, and an expanded interfascicular area [19].

Our study revealed similar changes within the ligament and showed significant variations within the population of studied dogs. Evaluation of other intra-articular ligaments (*i.e.*, FHL and CaCL) did not uncover any significant differences within their histological structure when compared within the population of examined dogs. The CaCLs in our study showed mild structural changes with a light degree of chondroid metaplasia. This result agrees with those in a previous study, which was limited to the description and comparison of CaCLs without comparison to the CCL structure [34]. The FHLs had the typical structure of ligaments without any sign of metaplasia apart from its presence at the attachment areas. Based on these results, it can be concluded that there are differences in the structure of intra-articular ligaments within the same and between distant joints.

The structural changes within the CCLs (*e.g.*, chondroid metaplasia of the fibroblasts and an increased amount of extracellular matrix) were strongly correlated with an increasing TPA and a narrowing ICN, which corresponds with observations in previous studies comparing the structural changes in the CCLs in different breeds of dogs [5,19,36]. However, chondroid metaplasia within the ligament may be considered a physiologic feature due to the athletic nature of dogs included in the study [5]. Furthermore, it was hypothesized that the observed microscopic changes could be related to impingement of the central part of the CCL and CaCL on the ICN [19,36]. Our findings suggest that increasing the tibial plateau slope increases the mechanical load of the CCL, which subsequently increases the compression and tension forces acting through the ligamentous tissues. This consequently leads to structural changes within the ligament as described in the study of Hayashi *et al.* [19] in which compressive forces acting through the tissue created this physiological adaptation. The adaptations are characterized by an increase in the glycosaminoglycan content, resulting in an increase in water content and osmotic pressure. Subsequently, such changes create pressure on the collagen network, which increases the

ability to resist the compression. The process is followed by the development of fibrocartilage with different mechanical properties than that in a physiological ligamentous structure [36].

Crimping of collagen fibers is another feature of the CCL, and one that is considered pathological as well as an adaptation to forces acting through the ligament [5,7,19,36]. We have also revealed crimp development in some investigated specimens. The crimps in the tendinous tissue were previously described as a feature of healthy collagen fibers and which diminishes with increased shear and tension forces as well as during the healing process [5]. However, an increased amount of crimp in the collagen fibers should rather be considered as an artefact created during preparation of the ligament tissue samples.

Furthermore, CCLs showed striking structural changes compared to only mild morphological changes within the CaCLs. Modifications were mainly observed within the central part of ligaments. This finding further supports the biomechanical theory of forces creating high compression forces within the ligaments in areas where these two ligaments spiral around each other. Narrowing of the ICN further increases CCL impingement where it comes into direct contact with the femoral condyle. Considering the similarities in the structure of cruciate ligaments to the FHL, we expected comparable changes would occur. However, we did not detect any signs of chondroid metaplasia in examined samples of FHLs. We propose that different forces act through the FHL because of its location inside the hip joint. Nevertheless, the exact role of the FHL in adult dogs remains to be elucidated.

Immunohistochemical analysis of S-100 and MMP-2 levels demonstrated low expression in healthy ligaments. Increased expression was strongly correlated with increasing TPA (Table 2, Fig. 2) and narrowing ICN width (Fig. 3). The S-100 protein is generally localized in cells derived from the neural crest (Schwann cells, glial cells), chondrocytes, and adipocytes. Some authors consider S-100 as a marker of proliferation [35]. Its presence has been described as a substance in the perinuclear halo of metaplastic fibroblasts of the CCL [5]. MMP-2 is a zinc-dependent endopeptidase involved in a variety of functions including inflammation and extracellular matrix degradation [36]. It is widely expressed by most cell types and appears to be up-regulated in tissues with high tensional forces [12]. In addition, increased hydrostatic pressure (high water content within fibrocartilage) accelerates tissue degeneration by increasing metalloproteinase production. On the other hand, it is not clear whether biomechanical forces can exert a sustained effect on MMP expression within fibrocartilaginous tissue. Our results support the hypothesis that increased forces acting through ligamentous tissues lead to chondroid metaplasia and development of fibrocartilage clusters within the core part of the ligament. The expression of S-100 co-localizes with the cartilaginous metaplasia during chondrocyte differentiation,

while MMP-2 positivity suggests increased proliferation and degradation of extracellular components, resulting in the different biomechanical properties of the CCL.

Biomechanical studies have described cartilage as a tissue resilient to compression and tension forces, but weak in resistance to shear forces [24,39]. The cross-sections of the CCL's central part, where it spirals around the CaCL and ICN, exhibited the formation of cartilage clusters, which is likely due to compression and tensile stress. The CCL has a proximal-to-distal outward spiral of about 90°, particularly in stifle flexion. This twist is caused by two distinct bands, a craniomedial band and a slightly larger caudolateral band [40]. The craniomedial band is taut in both extension and flexion, whereas the caudolateral part is taut in extension only. Therefore, the greater the tension, the higher the compression forces acting on the twisted part, thereby initiating fibrocartilage formation [36]. It is important to also consider the development of shear forces acting through the ligament at the level of its spiral [24,27]. The part of the ligament with differentiating fibrocartilage then becomes '*Locus minoris resistentiae*' to its micro-rupture and subsequent failure of the CCL. Our observations are therefore in contradiction with the study of Comerford *et al.* [6], in which fibrocartilage development was considered as a physiological feature of the ligament under tensile stress. This study [6], however, did not take into account all forces acting through the ligament (*e.g.*, compression and shear forces).

In conclusion, we propose that an increased TPA and a narrow ICN probably lead to increased compression and shear forces within the ligament, subsequent development of cartilage within the ligament, and susceptibility of the ligament to rupture. Increased expression of MMP-2, possible micro-ruptures, and disruption of normal structure within the ligament can further exacerbate the condition and trigger a cascade of inflammatory reactions within the joint.

## Conflict of Interest

The authors declare no conflicts of interest.

## References

1. **Anderst WJ, Tashman S.** The association between velocity of the center of closest proximity on subchondral bones and osteoarthritis progression. *J Orthop Res* 2009, **27**, 71-77.
2. **Barrett JG, Hao Z, Graf BK, Kaplan LD, Heiner JP, Muir P.** Inflammatory changes in ruptured canine cranial and human anterior cruciate ligaments. *Am J Vet Res* 2005, **66**, 2073-2080.
3. **Bossard MJ, Tomaszek TA, Thompson SK, Amegadzie BY, Hanning CR, Jones C, Kurdyla JT, McNulty DE, Drake FH, Gowen M, Levy MA.** Proteolytic activity of human osteoclast cathepsin K. Expression, purification, activation, and substrate identification. *J Biol Chem* 1996, **271**,

- 12517-12524.
4. **Comerford EJ, Innes JF, Tarlton JF, Bailey AJ.** Investigation of the composition, turnover, and thermal properties of ruptured cranial cruciate ligaments of dogs. *Am J Vet Res* 2004, **65**, 1136-1141.
  5. **Comerford EJ, Tarlton JF, Avery NC, Bailey AJ, Innes JF.** Distal femoral intercondylar notch dimensions and their relationship to composition and metabolism of the canine anterior cruciate ligament. *Osteoarthritis Cartilage* 2006, **14**, 273-278.
  6. **Comerford EJ, Tarlton JF, Innes JF, Johnson KA, Amis AA, Bailey AJ.** Metabolism and composition of the canine anterior cruciate ligament relate to differences in knee joint mechanics and predisposition to ligament rupture. *J Orthop Res* 2005, **23**, 61-66.
  7. **Comerford EJ, Tarlton JF, Wales A, Bailey AJ, Innes JF.** Ultrastructural differences in cranial cruciate ligaments from dogs of two breeds with a differing predisposition to ligament degeneration and rupture. *J Comp Pathol* 2006, **134**, 8-16.
  8. **Cook JL.** Cranial cruciate ligament disease in dogs: biology versus biomechanics. *Vet Surg* 2010, **39**, 270-277.
  9. **de Rooster H, de Bruin T, van Bree H.** Morphologic and functional features of the canine cruciate ligaments. *Vet Surg* 2006, **35**, 769-780.
  10. **Dennler R, Kipfer NM, Tepic S, Hassig M, Montavon PM.** Inclination of the patellar ligament in relation to flexion angle in stifle joints of dogs without degenerative joint disease. *Am J Vet Res* 2006, **67**, 1849-1854.
  11. **Duval JM, Budsberg SC, Flo GL, Sammarco JL.** Breed, sex, and body weight as risk factors for rupture of the cranial cruciate ligament in young dogs. *J Am Vet Med Assoc* 1999, **215**, 811-814.
  12. **Fitch RB, Montgomery RD, Milton JL, Garrett PD, Kincaid SA, Wright JC, Terry GC.** The intercondylar fossa of the normal canine stifle an anatomic and radiographic study. *Vet Surg* 1995, **24**, 148-155.
  13. **Fujita Y, Hara Y, Nezu Y, Schulz KS, Tagawa M.** Proinflammatory cytokine activities, matrix metalloproteinase-3 activity, and sulfated glycosaminoglycan content in synovial fluid of dogs with naturally acquired cranial cruciate ligament rupture. *Vet Surg* 2006, **35**, 369-376.
  14. **Galloway RH, Lester SJ.** Histopathological evaluation of canine stifle joint synovial membrane collected at the time of repair of cranial cruciate ligament rupture. *J Am Anim Hosp Assoc* 1995, **31**, 289-294.
  15. **Gambardella PC, Wallace LJ, Cassidy F.** Lateral suture technique for management of anterior cruciate ligament rupture in dogs: a retrospective study. *J Am Anim Hosp Assoc* 1981, **17**, 33-38.
  16. **Guerrero TG, Geyer H, Hässig M, Montavon PM.** Effect of conformation of the distal portion of the femur and proximal portion of the tibia on the pathogenesis of cranial cruciate ligament disease in dogs. *Am J Vet Res* 2007, **68**, 1332-1337.
  17. **Halleen JM, Räsänen S, Salo JJ, Reddy SV, Roodman GD, Hentunen TA, Lehenkari PP, Kaija H, Vihko P, Väänänen HK.** Intracellular fragmentation of bone resorption products by reactive oxygen species generated by osteoclastic tartrate-resistant acid phosphatase. *J Biol Chem* 1999, **274**, 22907-22910.
  18. **Hayashi K, Kim SY, Lansdowne JL, Kapatkin A, Déjardin LM.** Evaluation of a collagenase generated osteoarthritis biomarker in naturally occurring canine cruciate disease. *Vet Surg* 2009, **38**, 117-121.
  19. **Hayashi K, Manley PA, Muir P.** Cranial cruciate ligament pathophysiology in dogs with cruciate disease: a review. *J Am Anim Hosp Assoc* 2004, **40**, 385-390.
  20. **Innes JF, Bacon D, Lynch C, Pollard A.** Long-term outcome of surgery for dogs with cranial cruciate ligament deficiency. *Vet Rec* 2000, **147**, 325-328.
  21. **Kafienah W, Brömme D, Buttle DJ, Croucher LJ, Hollander AP.** Human cathepsin K cleaves native type I and II collagens at the N-terminal end of the triple helix. *Biochem J* 1998, **331**, 727-732.
  22. **Kim SE, Pozzi A, Kowaleski MP, Lewis DD.** Tibial osteotomies for cranial cruciate ligament insufficiency in dogs. *Vet Surg* 2008, **37**, 111-125.
  23. **Kipfer NM, Tepic S, Damur DM, Guerrero T, Hässig M, Montavon PM.** Effect of tibial tuberosity advancement on femorotibial shear in cranial cruciate-deficient stifles. An in vitro study. *Vet Comp Orthop Traumatol* 2008, **21**, 385-390.
  24. **Kirkby KA, Lewis DD.** Canine hip dysplasia: reviewing the evidence for nonsurgical management. *Vet Surg* 2012, **41**, 2-9.
  25. **Kowaleski MP, Apelt D, Mattoon JS, Litsky AS.** The effect of tibial plateau leveling osteotomy position on cranial tibial subluxation: an in vitro study. *Vet Surg* 2005, **34**, 332-336.
  26. **Krayer M, Rytz U, Oevermann A, Doherr MG, Forterre F, Zurbriggen A, Spreng DE.** Apoptosis of ligamentous cells of the cranial cruciate ligament from stable stifle joints of dogs with partial cranial cruciate ligament rupture. *Am J Vet Res* 2008, **69**, 625-630.
  27. **Leunig M, Beck M, Stauffer E, Hertel R, Ganz R.** Free nerve endings in the ligamentum capitis femoris. *Acta Orthop Scand* 2000, **71**, 452-454.
  28. **Morris E, Lipowitz AJ.** Comparison of tibial plateau angles in dogs with and without cranial cruciate ligament injuries. *J Am Vet Med Assoc* 2001, **218**, 363-366.
  29. **Muir P, Hayashi K, Manley PA, Colopy SA, Hao Z.** Evaluation of tartrate-resistant acid phosphatase and cathepsin K in ruptured cranial cruciate ligaments in dogs. *Am J Vet Res* 2002, **63**, 1279-1284.
  30. **Muir P, Schamberger GM, Manley PA, Hao Z.** Localization of cathepsin K and tartrate-resistant acid phosphatase in synovium and cranial cruciate ligament in dogs with cruciate disease. *Vet Surg* 2005, **34**, 239-246.
  31. **Pozzi A, Kowaleski MP, Apelt D, Meadows C, Andrews CM, Johnson KA.** Effect of medial meniscal release on tibial translation after tibial plateau leveling osteotomy. *Vet Surg* 2006, **35**, 486-494.
  32. **Reif U, Hulse DA, Hauptman JG.** Effect of tibial plateau leveling on stability of the canine cranial cruciate-deficient stifle joint: an in vitro study. *Vet Surg* 2002, **31**, 147-154.
  33. **Riitano MC, Pfister H, Engelhardt P, Neumann U, Reist M, Zurbriggen A, Stoffel M, Peel J, Jungi T, Schawalder P, Spreng DE.** Effects of stimulus with proinflammatory mediators on nitric oxide production and matrix metalloproteinase activity in explants of cranial cruciate

- ligaments obtained from dogs. *Am J Vet Res* 2002, **63**, 1423-1428.
34. **Shahar R, Milgram J.** Biomechanics of tibial plateau leveling of the canine cruciate-deficient stifle joint: a theoretical model. *Vet Surg* 2006, **35**, 144-149.
  35. **Trumble TN, Billingham RC, McIlwraith CW.** Correlation of prostaglandin E2 concentrations in synovial fluid with ground reaction forces and clinical variables for pain or inflammation in dogs with osteoarthritis induced by transection of the cranial cruciate ligament. *Am J Vet Res* 2004, **65**, 1269-1275.
  36. **Vasseur PB, Pool RR, Amoczky SP, Lau RE.** Correlative biomechanical and histologic study of the cranial cruciate ligament in dogs. *Am J Vet Res* 1985, **46**, 1842-1854.
  37. **Warzee CC, DeJardin LM, Amoczky SP, Perry RL.** Effect of tibial plateau leveling on cranial and caudal tibial thrusts in canine cranial cruciate-deficient stifles: an in vitro experimental study. *Vet Surg* 2001, **30**, 278-286.
  38. **Whitehair JG, Vasseur PB, Willits NH.** Epidemiology of cranial cruciate ligament rupture in dogs. *J Am Vet Med Assoc* 1993, **203**, 1016-1019.
  39. **Wingfield C, Amis AA, Stead AC, Law HT.** Comparison of the biomechanical properties of rottweiler and racing greyhound cranial cruciate ligaments. *J Small Anim Pract* 2000, **41**, 303-307.
  40. **Zachos TA, Amoczky SP, Lavagnino M, Tashman S.** The effect of cranial cruciate ligament insufficiency on caudal cruciate ligament morphology: An experimental study in dogs. *Vet Surg* 2002, **31**, 596-603.